American Mineralogist, Volume 85, pages 259–262, 2000

LETTER

High-pressure synthesis of $Na_2Mg_6Si_6O_{18}(OH)_2$—a new hydrous silicate phase isostructural with aenigmatite

HEXIONG YANG AND JÜRGEN KONZETT

Geophysical Laboratory and Center for High Pressure Research, Carnegie Institution of Washington, 5251 Broad Branch Road, N.W., Washington, D.C. 20015-1305, U.S.A.

ABSTRACT

A new hydrous phase, $Na_2Mg_6Si_6O_{18}(OH)_2$, which is isostructural with aenigmatite, was synthesized at 10 GPa and 1250 °C and its structure studied with X-ray diffraction data collected from a twinned crystal on a CCD diffractometer. The unit-cell parameters are a = 10.2925(9), b = 10.7052(9), c = 8.8027(10) Å, α = 105.280(2), β = 96.712(2), γ = 125.256(2)°, and V = 718.1(5) Å^3. The structure refinement indicates that O4 and O14, the only 2 O atoms that are not bonded to Si, are protonated. The presence of OH in the structure is confirmed by an unpolarized Raman spectrum. Compared to anhydrous sodic phases with the aenigmatite-type structure, silicate chains in hydrous $Na_2Mg_6Si_6O_{18}(OH)_2$ are more kinked, resulting in relatively long average Na-O distances.

INTRODUCTION

Aenigmatite-group minerals, albeit minor, are relatively common constituents of a variety of volcanic, plutonic, metamorphic, and metasomatic rocks; they also occur in meteorites (e.g., Deer et al. 1997). The composition of aenigmatite-group minerals conforms to a general formula $A_2B_6T_6O_{20}$, where A cations are sevenfold or eightfold-coordinated Na and Ca, B octahedrally coordinated Fe^{2+}, Fe^{3+}, Mg, Al, Cr, Ti, and Sb^{5+}, and T tetrahedrally coordinated Si, Al, B, and Be. There are two crystallographically distinct A sites (M8 and M9), seven B sites (M1-M7), and six T sites (T1-T6) in the aenigmatite-type structure. Eight members of the aenigmatite group have been identified to date in natural rocks (e.g., Burt 1994; Jensen 1996; Deer et al. 1997), the most common of which is aenigmatite, $Na_2(Fe^{2+}{}_5\,Ti)Si_6O_{20}$, whereas the B-, Be-, Sb-, and/or Cr-bearing members (welshite, høgtuvaite, serendibite, and krinovite) are rare. Kunzman (1999) thoroughly reviewed the minerals of the aenigmatite-rhönite group. In addition, several high-temperature synthetic phases have been reported to possess the aenigmatite-type structure, such as SFCA ($Ca_{2.3}Mg_{0.8}Al_{1.5}Fe_{8.3}Si_{1.1}O_{20}$) (Hamilton et al. 1989; Mumme et al. 1998), CSVA [$Ca_2Al_2(Al,V,Mg)_4(V,Al,Fe,Mn,Ti,Mg)_2(Si,Al)_4O_{20}$] (Arakcheeva and Ivanov 1993), CSTA ($Ca_{2.14}Mg_{2.72}Al_{4.32}Ti_{2.96}Si_{1.80}O_{20}$) (Arakcheeva 1995), and NaMgFe-germanate [$Na_2(Mg,Fe)_6(Ge,Fe)_6O_{20}$] (Barbier 1995). Recently, Gasparik et al. (1999) synthesized a phase of the composition $Na_2Mg_{4+x}Fe^{3+}{}_{2-2x}Si_{6+x}O_{20}$ with x = 0.25–0.60 at 13–14 GPa and 1450–1600 °C and found it to be isostructural with aenigmatite. This result suggests that the stability of aenigmatite-group minerals could be much greater than was evident so far and phases with the aenigmatite-type structure could play a more important role in the deeper mantle than in the Earth's crust. Here we report results of the single-crystal structure analysis of a hydrous silicate phase, $Na_2Mg_6Si_6O_{18}(OH)_2$, synthesized at high pressure, which represents the first aenigmatite-type structure containing OH.

EXPERIMENTAL PROCEDURES

The $Na_2Mg_6Si_6O_{18}(OH)_2$ sample was synthesized in a multi-anvil apparatus at 10.0 GPa and 1250 °C for 10 hours. The starting composition in weight percent of SiO_2 (46.1), Al_2O_3 (2.6), MgO (28.9), Na_2O (20.9), and H_2O (1.5) was designed to study high pressure breakdown products of amphibole. The starting material was prepared from high purity (99.99%+) SiO_2, Al_2O_3, MgO, and Na_2CO_3 with water added to the anhydrous and decarbonated oxide mix as brucite. After the run, the Pt_{100} sample container was embedded in epoxy resin and ground to expose the center of the charge, in which two different phases were found: hydrous $Na_2Mg_6Si_6O_{18}(OH)_2$ forming isometric crystals up to ~80 µm in diameter concentrated at the cooler end of the capsule and anhydrous $Na_2Mg_2Si_2O_7$ forming large blocky crystals up to ~300 µm in the largest dimension. The phase composition was determined with an electron microprobe (JEOL superprobe) using analytical conditions of 15 kV and 5 nA with a rastered beam size of 20 µm to minimize electron beam damage. Pure SiO_2, MgO, Al_2O_3 and synthetic omphacite were used as standards with 20 s on peaks and 10 s on backgrounds of the X-ray lines. The average composition of $Na_2Mg_6Si_6O_{18}(OH)_2$ from 12 measurements was found to be in wt% SiO_2 52.5(3), Al_2O_3 3.6(2), MgO 31.6(3), and Na_2O 9.2(2) with a total oxide sum of 96.9(6) wt%. Given the results of the structural analysis, the chemical formula was calculated on the basis of 18 O atoms + 2 OH, resulting in $Na_{2.02}Mg_{5.35}Al_{0.48}Si_{5.96}O_{18}(OH)_2$ with a stoichiomeric H_2O content of 2.6 wt%.

Raman spectra were recorded with a Dilor XY confocal mi-

*E-mail: yang@gl.ciw.edu

0003-004X/00/0001–0259$05.00

croRaman spectrometer equipped with a cryogenic Wright Model CCD detector. The excitation source was the 514 nm line of a coherent Innova Model 90-5 Ar^+ laser operating at 150 mW.

Based on optical examination, a nearly cube-shaped crystal (0.07 mm × 0.07 mm × 0.06 mm) was mounted on a Bruker Smart CCD X-ray diffractometer equipped with graphite-monochromatized Mo$K\alpha$ radiation ($\lambda = 0.71069$ Å). A hemisphere of three-dimensional X-ray diffraction data ($0° < 2\theta < 54°$) was collected with frame widths of 0.3° in ω and 30 s counting time per frame. The data were analyzed to locate peaks for the determination of the unit-cell parameters. An initial calculation of unit-cell parameters yielded a *C*-centered monoclinic cell similar to those reported for twinned aenigmatite-group phases (Cannillo et al. 1971; Bonaccorsi et al. 1990; Barbier 1995; Gasparik et al. 1999). Thus, the data were re-indexed with two twin components; all reflections were indexed to one or both components based on the unit-cell parameters: $a = 8.8027(9)$, $b = 9.6609(9)$, $c = 10.2925(10)$ Å, $\alpha = 64.802(2)$, $\beta = 83.288(2)$, and $\gamma = 65.383(2)°$. The twin law relating the twin components is, by row, [0, 1, –1/2; 1, 0 –1/2; 0, 0, –1]. The separate orientation matrices were then employed to integrate intensity data using the Siemens program SAINT. An empirical correction for X-ray absorption was made using the program SADABS (incorporated in SAINT). The X-ray intensity data were also corrected for the twin components with the program UNTWIN (incorporated in SAINT). Note that the reduced unit cell obtained above is different from that customarily used in the literature for the aenigmatite-group phases. To keep consistency with the previous work, we adopted the customary unit cell in the structure refinement [$a = 10.2925(10)$, $b = 10.7052(10)$, $c = 8.8027(9)$ Å, $\alpha = 105.280(2)$, $\beta = 96.712(2)$, $\gamma = 125.256(2)°$, and $V = 718.1(5)$ Å^3], which can be related to the reduced unit cell through the transformation matrix (by row): (0 0 1), (0 1 $\bar{1}$), ($1\bar{}$ 0 0).

The structure of the $Na_2(Mg_{5.35}Al_{0.48})Si_{5.96}O_{18}(OH)_2$ phase was refined in space group $P1\bar{}$ using SHELX97. All cation sites were assumed to be fully occupied throughout the refinements, with Na in the A sites, Mg in the B sites, and Si in the T sites. The small amount of Al was assigned to the M7 site, as previous studies suggested that this site is favored by small, high-valence cations

TABLE 1. Atomic coordinates and equivalent isotropic displacement parameters

	x	y	z	U_{eq}
M1	0	0	½	0.0130(5)
M2	0	½	0	0.0174(5)
M3	0.3139(5)	0.8498(3)	0.1782(3)	0.0095(4)
M4	0.7687(5)	0.8195(3)	0.1512(3)	0.0086(4)
M5	0.5949(5)	0.9407(4)	0.0617(4)	0.0085(2)
M6	0.0966(5)	0.9420(4)	0.0534(4)	0.0135(3)
M7	0.9900(3)	0.7309(2)	0.2680(2)	0.0078(2)
M8	0.2088(5)	0.6334(4)	0.3899(4)	0.0151(5)
M9	0.6620(6)	0.6099(4)	0.3672(4)	0.0155(5)
T1	0.4765(4)	0.2333(3)	0.3335(3)	0.0084(4)
T2	0.9804(4)	0.2299(3)	0.3428(3)	0.0086(4)
T3	0.7880(3)	0.3385(3)	0.2375(3)	0.0060(4)
T4	0.2780(3)	0.3398(3)	0.2243(3)	0.0060(4)
T5	0.6478(2)	0.9495(2)	0.4428(2)	0.0078(2)
T6	0.3563(2)	0.5596(2)	0.0455(2)	0.0079(2)
O1	0.3516(9)	0.0676(7)	0.1688(7)	0.0108(11)
O2	0.8517(9)	0.0627(7)	0.1745(7)	0.0109(11)
O3	0.5577(10)	0.9605(7)	0.2931(7)	0.0104(10)
O4	0.0267(10)	0.9456(8)	0.2735(8)	0.0195(13)
O5	0.2398(10)	0.8748(7)	0.3858(7)	0.0137(12)
O6	0.7537(10)	0.8856(7)	0.3865(8)	0.0132(12)
O7	0.5047(8)	0.8015(6)	0.4992(7)	0.0091(9)
O8	0.9565(8)	0.7835(6)	0.4900(7)	0.0105(10)
O9	0.8914(8)	0.3152(6)	0.3728(6)	0.0110(10)
O10	0.3992(8)	0.3323(7)	0.3563(6)	0.0075(10)
O11	0.6578(8)	0.1653(6)	0.0655(7)	0.0073(11)
O12	0.1560(8)	0.1641(6)	0.0585(7)	0.0068(11)
O13	0.5318(9)	0.7163(7)	0.0378(7)	0.0098(10)
O14	0.0617(9)	0.7323(7)	0.0603(7)	0.0097(10)
O15	0.2426(9)	0.6091(7)	0.1100(7)	0.0066(11)
O16	0.7484(9)	0.6084(7)	0.1260(7)	0.0082(11)
O17	0.4032(9)	0.5036(7)	0.1907(7)	0.0104(9)
O18	0.9335(9)	0.5048(7)	0.2196(7)	0.0115(10)
O19	0.1594(8)	0.3645(6)	0.3150(6)	0.0123(11)
O20	0.6705(8)	0.3637(6)	0.3367(6)	0.0066(9)
H1	0.1290	0.0486	0.3422	
H2	0.0241	0.3381	0.0489	

TABLE 2. Selected interatomic distances for synthetic $Na_2Mg_6Si_6O_{18}(OH)_2$

T1	O1	1.574 (6)	M4	O2	2.159 (6)
T1	O7	1.628 (6)	M4	O4	2.112 (6)
T1	O10	1.641 (5)	M4	O6	2.060 (7)
T1	O20	1.639 (5)	M4	O12	2.095 (6)
T1	Avg	1.621	M4	O13	1.976 (5)
			M4	O16	2.092 (6)
T2	O2	1.600 (6)	M4	Avg	2.082
T2	O8	1.614 (5)			
T2	O9	1.625 (5)	M5	O1	2.156 (6)
T2	O19	1.661 (6)	M5	O2	2.096 (6)
T2	Avg	1.625	M5	O3	2.095 (6)
			M5	O11	2.088 (6)
T3	O9	1.667 (5)	M5	O11	2.133 (6)
T3	O11	1.645 (5)	M5	O13	2.034 (6)
T3	O18	1.601 (6)	M5	Avg	2.100
T3	O20	1.672 (5)			
	Avg	1.646	M6	O1	2.076 (6)
			M6	O2	2.130 (6)
T4	O10	1.655 (5)	M6	O4	2.142 (6)
T4	O12	1.626 (5)	M6	O12	2.071 (6)
T4	O17	1.605 (6)	M6	O12	2.102 (6)
T4	O19	1.640 (5)	M6	O14	2.079 (6)
Avg	1.632		M6	Avg	2.100
T5	O3	1.591 (5)	M7	O4	2.089 (7)
T5	O5	1.655 (6)	M7	O5	2.005 (6)
T5	O6	1.646 (6)	M7	O8	2.014 (6)
T5	O7	1.679 (5)	M7	O14	2.051 (6)
T5	Avg	1.643	M7	O16	2.028 (5)
			M7	O18	2.037 (6)
T6	O13	1.635 (5)	M7	Avg	2.037
T6	O15	1.638 (5)			
T6	O16	1.621 (6)	M8	O5	2.425 (6)
T6	O17	1.679 (5)	M8	O7	2.348 (5)
Avg	1.643		M8	O9	2.506 (6)
			M8	O9	3.011 (6)
M1	O4 (×2)	2.023 (6)	M8	O15	2.496 (5)
M1	O6 (×2)	2.026 (6)	M8	O18	2.364 (5)
M1	O8 (×2)	2.065 (5)	M8	O19	2.492 (6)
M1	Avg	2.038	M8	O20	2.560 (5)
			M8	Avg	2.525
M2	O14 (×2)	2.067 (6)			
M2	O15 (×2)	2.002 (5)	M9	O6	2.472 (6)
M2	O18 (×2)	2.123 (6)	M9	O8	2.341 (5)
M2	Avg	2.064	M9	O10	2.582 (6)
			M9	O10	2.592 (7)
M3	O1	2.158 (6)	M9	O16	2.396 (6)
M3	O3	2.017 (6)	M9	O17	2.325 (5)
M3	O5	2.073 (7)	M9	O19	3.016 (6)
M3	O11	2.174 (6)	M9	O20	2.632 (6)
M3	O14	2.076 (5)	M9	Avg	2.545
M3	O15	2.107 (6)			
M3	Avg	2.101			

(e.g., Cannillo et al. 1971; Bonaccorsi et al. 1990; Gasparik et al. 1999). The smallest U_{eq} value for M7 among all B-type cations (Table 1) is in keeping with such an assignment. The difference Fourier maps at the convergence of the refinement revealed two low positive peaks: one (0.94 e/Å^3) at a distance of ~1.00 Å from O4 and the other (0.75 e/Å^3) at a distance of ~0.93 Å from O14. These two positions were thus assumed to be occupied by H. Because a refinement of the H positions was unsuccessful, a riding model was adopted, with H1 on O4 and H2 on O14. The resulting R_1 and wR_2 factors are 0.042 and 0.112, respectively, for 4906 reflections [$I > 4\sigma(I)$] with anisotropic refinements for all atoms but H. The determined ratio of two twin components is 0.54:0.46. Final atomic coordinates and equivalent isotropic displacement parameters are presented in Table 1 and selected interatomic distances in Table 2.

Results and discussion

The crystal structure of the $Na_2Mg_6Si_6O_{18}(OH)_2$ phase, which is similar to that of the aenigmatite-group phases, is characterized by two types of polyhedral layers stacking alternately along [011]: One layer is formed by slabs of B-octahedra (M3-M7) linked by bands of A-polyhedra (M8 and M9) and the other by open-branched vierer single tetrahedral chains (Liebau 1985) connected by isolated B-octahedra (M1 and M2) (Fig. 1). However, all previously studied natural or synthetic phases with the aenigmatite-type structure are anhydrous, whereas our sample clearly contains OH in the structure, as indicated by the measured Raman spectrum (Fig. 2).

The $Na_2Mg_6Si_6O_{18}(OH)_2$ structure contains 20 independent O atoms, among which 18 O atoms are bonded to Si cations forming the $[Si_6O_{18}]^{12-}$ branched pyroxene-type chains. The two remaining (O4 and O14) are bonded to Mg only. As suggested by the structure refinement, the two non-Si-bonded O atoms are most likely to be hydroxyl. This observation is consistent with the bond-valence calculation (Brown 1981), which shows that O4 and O14 are the most underbonded, with bond valences of 1.35 and 1.41, respectively. The location of the O-H groups in the $Na_2Mg_6Si_6O_{18}(OH)_2$ structure contrasts with the hypothesis that a possible crystal-chemical mechanism for the introduction of O-H groups in the aenigmatite structure may involve the tetrahedral sites (Oberti, personal communication). The presence of two crystallographically distinct O-H positions in the $Na_2Mg_6Si_6O_{18}(OH)_2$ structure is consistent with the Raman spectrum, which exhibits a peak at 3556 cm^{-1} with a shoulder at 3583 cm^{-1} (Fig. 2). The high frequencies of the O-H stretching vibrations point to rather weak hydrogen bonding, with O-H···O distances greater than 3.0 Å (Nakamoto et al. 1955). The structure analysis indicates that the O4-H and O14-H hydroxyl anions could be involved in weak hydrogen bonding with O10 and O19 atoms, respectively (O4-O10 = 3.43 Å and O14-O19 = 3.30 Å).

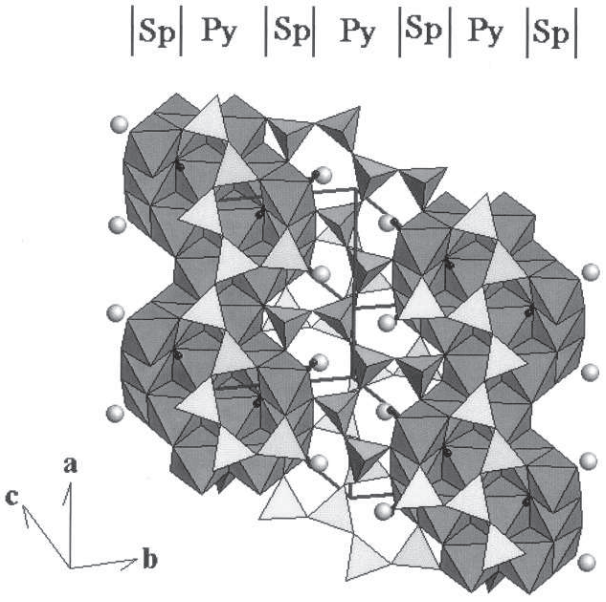

Figure 1. The crystal structure of $Na_2Mg_6Si_6O_{18}(OH)_2$. All octahedra are occupied by Mg and tetrahedra by Si. The large spheres represent Na cations and small black ones represent H. The spinel- and pyroxene-type slabs are labeled as "Sp" and "Py", respectively.

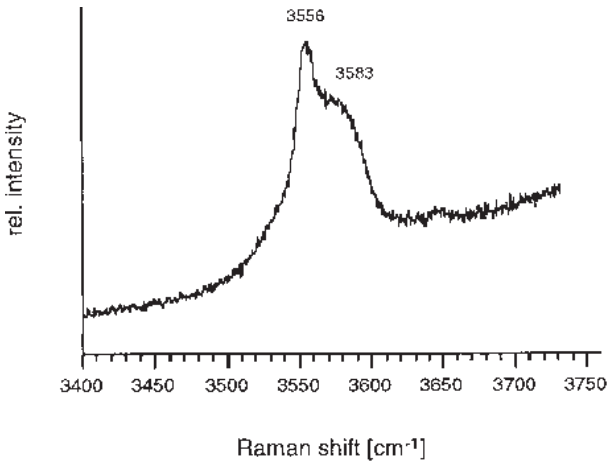

Figure 2. The unpolarized Raman spectrum of synthetic $Na_2Mg_6Si_6O_{18}(OH)_2$ in the OH-stretching region.

Another notable difference between the structure of $Na_2Mg_6Si_6O_{18}(OH)_2$ and the structures of sodic aenigmatite-group phases with silicate chains lies in the coordination environments of the two Na atoms. In the structures of $Na_2(Fe_5Ti)[Si_6O_{18}]O_2$ (aenigmatite, Cannillo et al. 1971), $Na_2(Mg_4Cr_2)[Si_6O_{18}]O_2$ (krinovite, Bonaccorsi et al. 1989), and $Na_2Mg_{4+x}Fe^{3+}_{2-2x}Si_{6+x}O_{20}$ (x = 0.25–0.60; Gasparik et al. 1999), all Na-O distances are within 3.0 Å; the longest Na-O length within the M8 polyhedron (M8-O9) ranges from 2.943(6) Å in $Na_2Mg_{4+x}Fe^{3+}_{2-2x}Si_{6+x}O_{20}$ to 2.965(9) Å in krinovite, whereas the longest Na-O distance within the M9 polyhedron (M9-O19) ranges from 2.956(12) Å in krinovite to 2.968(6) Å in $Na_2Mg_{4+x}Fe^{3+}_{2-2x}Si_{6+x}O_{20}$. However, the M8-O9 and M9-O19 distances in $Na_2Mg_6Si_6O_{18}(OH)_2$ are 3.011(6) and 3.016(6) Å, respectively. Due to this, the average Na-O distances for both

M8 and M9 polyhedra are longer than those in anhydrous sodic aenigmatite-group phases. The significantly longer M8-O9 and M9-O19 distances in $Na_2Mg_6Si_6O_{18}(OH)_2$ than as found in other sodic aenigmatite-group phases are associated with the increased kinking of the pyroxene-like silicate chains, as both O9 and O19, as well as O10 and O20, are bridging O atoms. The O19-O9-O20, O9-O19-O10, and O19-O10-O20 kinking angles are 148.98, 150.98, and 160.26°, respectively, in $Na_2Mg_6Si_6O_{18}(OH)_2$ whereas they are 149.48, 152.97, and 162.17° in krinovite and 151.52, 153.47, and 161.90° in $Na_2Mg_{4+x}Fe^{3+}{}_{2-2x}Si_{6+x}O_{20}$. The silicate chains in $Na_2Mg_6Si_6O_{18}(OH)_2$ are the most strongly kinked of all sodic aenigmatite-group phases. This observation might be related to the presence of weak hydrogen bonding. Though the O4-O10 and O14-O19 distances in $Na_2Mg_6Si_6O_{18}(OH)_2$ are relatively long (3.43 and 3.30 Å, respectively), they are, nevertheless, significantly shorter than the corresponding distances in krinovite (3.59 and 3.39 Å), in $Na_2Mg_{4+x}Fe^{3+}{}_{2-2x}Si_{6+x}O_{20}$ (3.53 and 3.38 Å), and in aenigmatite (3.66 and 3.52 Å).

The structure of aenigmatite phases can be described as an ordered 1:1 intergrowth of spinel- and pyroxene-type structural units with the spinel-type slabs containing M1, M2, and M7 octahedra plus T5 and T6 tetrahedra, and the pyroxene-type slabs containing M3-M6, M8, M9 octahedra plus T1-T4 tetrahedra (Bonaccorsi et al. 1990; Barbier 1995), see Figure 1. However, neither of these minerals has a suitable site for protonation. Hence, the pyroxene-spinal interface provides the locations for H^+ (Fig. 1), consistent with our refinements. The question then arises as to the possibility of OH^- in other aenigmatite-type minerals. Trace amounts of OH^- are to be expected because many nominally anhydrous minerals have OH^- as impurities (see Rossman 1988) and chain silicates are no exception. Population of the O4 and O14 sites in the natural minerals could occur through vacancies in the Na site, or $Fe^{3+} + O^{2-} = Fe^{2+} + OH^-$, or $Al^{3+} + OH^- = Si^{4+} + O^{2-}$ ….etc. One can also ask the converse question, given that aenigmatite minerals lack stoichometric H, why then does the present phase have such? The comparison to be made here may be the family of minerals known as dense hydrous magnesium silicates. Here, a myriad of structures exists because of the small sizes of Mg and Si, and tradeoffs in octahedral and tetrahedral coordination for both. The present phase can be viewed as an extention of the system to include Na.

Acknowledgments

We thank J.B. Parise at SUNY (Stony Brook) for providing us with their manuscript before its publication. Constructive comments and suggestions for improvement from two anonymous reviewers and R. Oberti are appreciated. We are benefited from valuable discussions with C.T. Prewitt, R.M. Hazen and L.W. Finger. X-ray diffraction work was supported by the NSF grant EAR-9805282, the Center for High Pressure Research, and by the Carnegie Institution of Washington. Diffraction data were obtained with a Bruker P4 CCD diffractometer purchased with grants from the W.M. Keck Foundation and the National Science Foundation.

References cited

Arakcheeva, A.V. (1995) Crystal structure of the baykovite mineral. Crystallography Report, 40, 220–227.

Arakcheeva, A.V. and Ivanov, I.T. (1993) Crystal structure of disomatic phase of variable composition $CaAl(Al,V,MI)_2(V,MII)(Si,Al)_2O_{10}$, where MI = Mg, MII = Al, Fe, Mn, Ti, Mg; its polytypic modifications and structural homologs. Crystallography Report, 38, 505–515.

Barbier, J. (1995) Structure refinement of $Na_2(Mg,Fe)_6[(Ge,Fe)_6O_{18}]O_2$, a new aenigmatite-analog. Zeitschrift für Kristallographie, 210, 19–23.

Bonaccorsi, E., Merlino, S., and Pasero, M. (1989) Crystal structure of the meteoritic mineral krinovite, $NaMg_2CrSi_3O_{10}$. Zeitschrift für Kristallographie, 187, 133–138.

——— (1990) Rhonite, structural and mircostructural features, crystal chemistry, and polysomatic relationships. European Journal of Mineralogy, 2, 203–218.

Brown, I.D. (1981) The bond-valence method: An empirical approach to chemical structure and bonding. In M. O'Keefe and A. Navrotsky, Eds., Structure and Bonding in Crystals, 2, p.1–30. Academic Press, New York.

Burt, D.M. (1994) Vector representation of some mineral compositions in the aenigmatite group, with special reference to høgtuvaite. Canadian Mineralogist, 32, 449–457.

Cannillo, E., Mazzi, F., Fang, J.H., Robinson, P.D., and Ohya, Y. (1971) The crystal structure of aenigmatite. American Mineralogist, 56, 427–446.

Deer, W.A., Howie, R.A., and Zussman, J. (1997) Rock-forming minerals. Single chain silicates. 668 p. Wiley, New York.

Gasparik, T., Parise, J.B., Reeder, R.J., Young, V.G., and Wilford, W.S. (1999) Composition, stability, and structure of a new member of the aenigmatite group, $Na_2Mg_{4+x}Fe^{3+}{}_{2-2x}Si_{6+x}O_{20}$, synthesized at 13–14 GPa. American Mineralogist, 84, 257–266.

Hamilton, J.D.G., Hoskins, B.F., Mumme, W.G., Borbidge, W.E., and Montague, M.A. (1989) The crystal structure and crystal chemistry of $Ca_{2.3}Mg_{0.8}Al_{1.5}Si_{1.1}Fe_{8.3}O_{22}$ (SFCA): solid solution limits and selected phase relationships of SFCA in the SiO_2-Fe_2O_3-CaO(-Al_2O_3) system. Neues Jahrbuch für Mineralogie, Abhandlungen 161, 1–26.

Jensen, B.B. (1996) Solid solution among members of the aenigmatite group. Mineralogical Magazine, 60, 982–986.

Kunzmann, T. (1999) The aenigmatite-rhönite mineral group. European Journal of Mineralogy, 11, 743–756.

Liebau, F. (1985) Structural Chemistry of Silicates, 104 p. Springer-Verlag, Berlin.

Mumme, W.G., Clout, J.M.F., and Gable, R.W. (1998) The crystal structure of SFCA-I, $Ca_{3.18}Fe^{3+}{}_{14.66}Al_{1.34}Fe^{2+}{}_{0.82}O_{28}$, a homologue of the aenigmatite structure type, and new crystal structure refinements of b-CFF, $Ca_{2.99}Fe^{3+}{}_{14.30}Fe^{2+}{}_{0.55}O_{25}$ and Mg-free SFCA, $Ca_{2.45}Fe^{3+}{}_{9.04}Al_{1.74}Fe^{2+}{}_{0.16}Si_{0.6}O_{20}$. Neues Jahrbuch für Mineralogie, Abhandlungen 173, 93–117.

Nakamoto, K., Margoshes, M., and Rundle, R.E. (1955) Stretching frequencies as a function of distances in hydrogen bonds. Journal of the American Chemical Society, 77, 6480–6486

Rossman, G.R. (1988) Vibrational spectroscopy of hydrous components. Mineralogical Society of America Reviews in Mineralogy, 18, 193–206.

Manuscript received March 31, 1999
Manuscript accepted September 14, 1999
Paper handled by Roberta Oberti